
PROBABILISTIC DEBIASING OF SCENE GRAPHS

A PREPRINT

Bashirul Azam Biswas
 Rensselaer Polytechnic Institute
 biswab@rpi.edu

Qiang Ji
 Rensselaer Polytechnic Institute
 jiq@rpi.edu

November 15, 2022

ABSTRACT

The quality of scene graphs generated by the state-of-the-art (SOTA) models is compromised due to the long-tail nature of the relationships and their parent object pairs. Training of the scene graphs is dominated by the majority relationships of the majority pairs and, therefore, the object-conditional distributions of relationship in the minority pairs are not preserved after the training is converged. Consequently, the biased model performs well on more frequent relationships in the marginal distribution of relationships such as ‘on’ and ‘wearing’, and performs poorly on the less frequent relationships such as ‘eating’ or ‘hanging from’. In this work, we propose virtual evidence incorporated within-triplet Bayesian Network (BN) to preserve the object-conditional distribution of the relationship label and to eradicate the bias created by the marginal probability of the relationships. The insufficient number of relationships in the minority classes poses a significant problem in learning the within-triplet Bayesian network. We address this insufficiency by embedding-based augmentation of triplets where we borrow samples of the minority triplet classes from its neighborhood triplets in the semantic space. We perform experiments on two different datasets and achieve a significant improvement in the mean recall of the relationships. We also achieve better balance between recall and mean recall performance compared to the SOTA de-biasing techniques of scene graph models.

1 Introduction

Any visual relationship in an image can be thought of as a triplet consisting of subject, relationship, and object. In recent years, these triplets are represented as a concise graph called Scene Graph (SG) [19] where the nodes represent the object labels and the edges represent labels of relationships. This compact representation has been proven useful for many downstream tasks such as image captioning [36], visual reasoning [24], and image generation [10]. Scene Graph Generation (SGG) has become one of the major computer vision research arenas, especially after the introduction of a large-scale crowd-annotated SG database named Visual Genome (VG) [11]. The distribution of triplets in VG images has two distinct characteristics: (1) presence of strong within-triplet prior, and (2) long-tail distribution of relationship. As shown in Figure 1 (a), the within-triplet prior dictates that ‘man’ will most likely be ‘eating’ a ‘pizza’ rather than be ‘on’ it and ‘window’ will most likely be ‘on’ the ‘building’ rather than ‘eating’ it. Zeller [42] has utilized this within-triplet prior as conditional probability of relationships given subject and object by proposing a frequency baseline in SGG task. On the other hand, the distribution of relationship labels suffers from a long-tailed nature and Tang [26] addressed this long-tailed issue by considering a causal interpretation of the biased prediction. We argue that these two seemingly different characteristics of the relationship distribution are inter-related. The abundance of the *head* classes of the relationship distribution in Figure 1 (c), such as ‘on’ and ‘wearing’, arises from the abundance of their parent subject and object lying in the *head* region of Figure 1 (b).

As indicated by [5], the long-tailed distribution exists both in relationship and object label. Since relationship labels are dependent on their object pair because of the within-triplet prior, the long-tail distribution of the relationship worsens due to the long-tail nature of the object pairs. VG images are crowd-collected which suffers from *selection bias* and crowd-annotated which suffers from *label-bias* [28]. To analyze such imbalances, we investigate the distribution of the object pair of the triplets in VG database. As shown in Figure 1 (b), ‘window-building’ and ‘man-shirt’ is the most

frequently annotated pairs and top 1% object pair covers 33% of all triplets. As a result, the dominant relationships in these *head* pairs, such as ‘on’ and ‘wearing’, dominate the marginal distribution of Figure 1 (c).

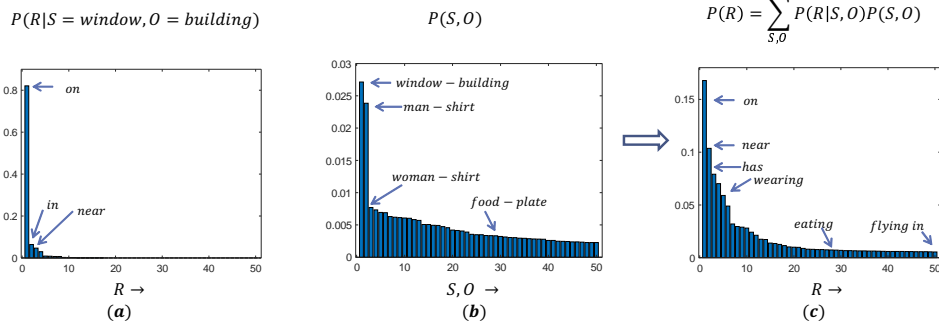


Figure 1: (a) Within-triplet dependency of relationship on its parent object pair; (b) long-tail nature of the pair statistics where 33% pair samples are originated from top 1% pairs; (c) long-tail nature of the relationships showing dominance of ‘on’ and ‘wearing’. The skewness in (c) is an effect of skewness in (b). Since ‘on’, ‘near’ or ‘wearing’ dominates in these top 1% pairs, they become the majority relationships in (c) and many other relationships, such as ‘eating’ or ‘flying in’, which dominate in the tail pairs of (b) are suppressed in the training process.

In a deep-learning based SGG model, while training, samplers will sample more relationships from the *head* pairs and hence, the parameter updating will be dominated by the dominant relationship of the majority pairs. As a result, Maximum Likelihood Estimation (MLE) of the parameters are biased in such a way that the prediction almost always takes the more frequent value in the training dataset [26]. On top of that, because of sampling more triplets from the *head* pairs, the object-conditional representation of the relationship in the *tail* pairs will be lost in the training process. Therefore, various deep learning based models which attempt to implicitly capture such object-conditional representation in SGG task either by employing a loss function [44] or by employing a class-aware feed-forward network [4], fail to preserve the representation in the trained model and perform poorly on the tail region of the relationships.

Removing such ‘bad’ biases in the training dataset is not an easy task since in real life these biases do exist [26]. Re-sampling or re-weighting the minority classes while training [5, 7, 3] or modifying the biased prediction in the inference phase using causal intervention [26] remove such ‘bad biases’ along with some ‘good biases’ which are necessary to maintain the linguistic meaning of the triplets. Consequently, these approaches hurt the performance in the majority classes, namely *recall* which are masked by the improvement in the average class performance, namely *mean recall*. Keeping this in mind, we propose an inference-time post-processing methodology of removing bias which extracts information from the support of the minority relationships as well as hurt the majority classes less brutally. We propose a within-triplet Bayesian Network (BN) where we restore the object-conditional distribution of relationships and eradicate the bias introduced by the long-tailed marginal distribution of relationship.

Learning such small within-triplet Bayesian network from the training data is a seemingly trivial task where we can perform simple MLE of parameters by counting. However, because of restricting our training samples only belonging to some top- N_r classes based on the marginal probability of relationship, we sacrifice many information revealing triplets in the minority pairs. For example, in ‘man-pizza’ pair, we see there exist many interesting relationships such as ‘man biting pizza’ or ‘man consuming pizza’ which are semantically similar to one of the top- N_r valid triplets ‘man eating pizza’. This phenomenon is also a result of *label bias* [28] where the annotator chooses some labels over another for the same category of objects or relationships. We propose a novel method of borrowing samples from such invalid triplets into learning distribution of the valid triplets using embedding based augmentation.

Posterior inference is the most efficient probabilistic tool to combine domain-dependent prior with instance-dependent evidence and, to the best of our knowledge, no prior work in SGG literature formulates the problem of triplet generation as a posterior inference problem which combines both the prior and the evidence. The overview of our approach is illustrated in Figure 2. In summary, our contribution is proposing a posterior inference based post-processing method where we

- integrate the within-triplet priors with the evidence uncertainties generated by the measurement model and,

- introduce a simple yet novel learning scheme of the within-triplet network where we borrow samples from the semantically similar yet invalid triplet categories.

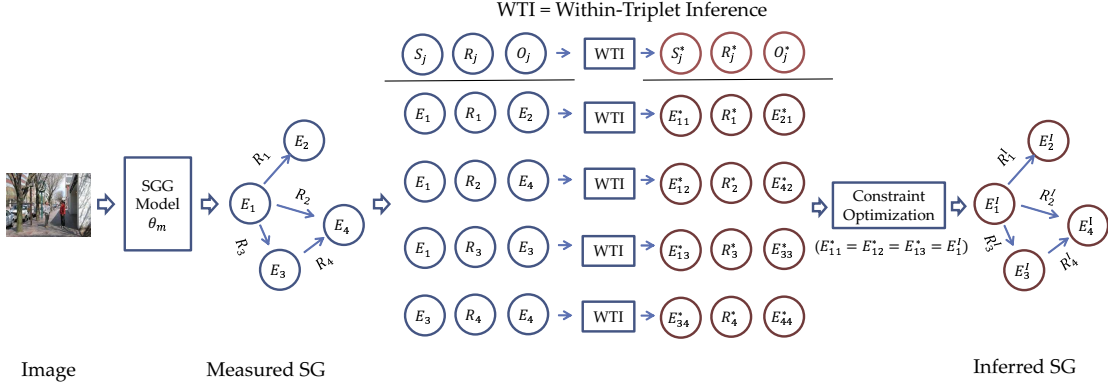


Figure 2: Overview of our proposed approach. For each testing image I , SGG baseline model θ_m generates physically connected triplets with associated uncertainties for subject, object, and relationship. Our within-triplet inference framework takes all the uncertainties as uncertain evidences and perform posterior inference to infer each triplet separately. Afterwards, a constrained optimization procedure is performed to resolve the conflict between object entities.

2 Related Works

Our proposed SGG model combines prior knowledge of triplets with the uncertain evidences of measurement models to address the long-tailed issue of relationships. Moreover, we learn the prior model using similarity of triplets in the language embedding space. Hence, we divide the related works into four major categories as following

Implicit prior and context incorporation: Global context of an image has been captured either by BiLSTM, Graph Neural Network (GNN), attentional Graph Convolution Network (aGCN), or Conditional Random Field (CRF) in [42, 31, 25, 33, 35]. Statistical information of triplets are encoded in [32, 2, 4]. Tang *et al.* composed a dynamic tree structure to capture relationships among objects [27]. Transformer based context capturing are adopted in [17, 41, 23, 13]. Within-triplet relations are incorporated in learnable modules as embeddings in [43, 29, 22]. All of these above methods extract the relational information from the training data whereas several other approaches [6, 39, 19, 16, 40] rely on external knowledge base such as ConceptNet [18].

Language models and ambiguity: Language and vision module are combined together to guide the training process in [19, 39, 9, 21]. Embeddings from phrasal context [38], word embedding based external knowledge incorporation [6, 40], and caption database [37] are used for supervision. Ambiguity of scene graph triplets are addressed in [34, 45, 12].

Long-tail distribution: An unbiased metric (*mean recall*) is proposed by [2, 27] to quantify the performance of the SGG models in the tail regions of the distribution. Several works addressed this long-tailedness in training through modified loss functions [17, 40] and re-weighting/re-sampling training samples [5, 7, 14, 15, 12, 3]. The most relevant to our work is the inference-time causal intervention proposed by Tang *et al.* [26] where they identified the ‘bad bias’ from counterfactual causality and attained significantly higher mean recall than other SOTA models. We, instead of applying causal intervention, resort to a graphical model based approach which can remove the ‘bad bias’ through uncertain evidence insertion into a Bayesian network while maintaining the ‘good bias’ by within-triplet prior incorporation.

Uncertain evidence: Incorporation of evidence uncertainty into belief networks has been discussed by Judea Pearl in [20]. A thorough discussion for interested readers can be found in [1]

3 Problem formulation

In scene graph generation database, every image I has an annotation of a scene graph $\mathcal{G}_I = (\mathcal{E}, \mathcal{R})$ where $\mathcal{E} = \{E_i, B_i\}_{i=1}^{N_E}$ contains the object classes E_i and their bounding boxes B_i whereas $\mathcal{R} = \{R_j(S_j, O_j)\}_{j=1}^{N_R}$ contains the

relationships of a scene graph. Each relationship R_j exists between its subject S_j and object O_j where $S_j, O_j \in \{E_i\}$. Now, in training any SGG model parameterized by θ , we can write the cost function as

$$\mathcal{J}(\theta) = \mathbb{E}_{\sim p(I, \mathcal{G})} L(I, \mathcal{G}, \theta) \approx \frac{1}{M} \sum_{i=1}^M L(I_i, \mathcal{G}_i, \theta) \quad (1)$$

where L is the loss function with parameter θ for a sample image I with associated scene graph \mathcal{G} and M is total number of images. Now, as shown in Figure 1, the distribution of scene graphs is skewed towards certain few categories of object pairs and their relationships. Therefore, while training, the cost function $\mathcal{J}(\theta)$ is driven by the *head* pairs while the relationships dominating in the *tail* pairs are ignored. As a result, many object-conditional distribution of relationships are not preserved after the training is converged. We propose a test-time post-processing method where the object-conditional distribution of relationships are restored by a within-triplet prior Bayesian network.

4 Posterior inference of Scene Graphs

4.1 Within-triplet Bayesian network

A scene graph is a collection of connected triplets and each triplet has three semantic components - subject (S), object (O), and their relationship (R) and two spatial components - subject bounding box B_s and object bounding box B_o . We consider the semantic components as random categorical variables and we aim to model their joint distribution $P(S, R, O)$. From our prior commonsense, we assume the following statements are true for any triplet,

1. Relationship label of a triplet depends on its subject and object $\implies S \rightarrow R \leftarrow O$;
2. Subject and object are independent, not given the relationship $\implies S \perp\!\!\!\perp O \mid R$;
3. Subject and object becomes dependent, given the relationship $\implies S \not\perp\!\!\!\perp O \mid R$

Based on these assumptions, we can build a Bayesian network of triplet, as shown in Figure 3 which encodes the joint distribution using chain rule as following

$$P(S, R, O) = P(S)P(O)P(R|S, O) \quad (2)$$

where $P(S)$ and $P(O)$ represent the marginal distribution of the parents S and O and $P(R|S, O)$ represents the conditional distribution of the relationship R given its parent subject and object. This Bayesian network encodes the prior joint distribution which resides within a triplet and hence we term it as within-triplet Bayesian network. In the next subsection, we discuss how we can debias the measurement probability of a relationship by incorporating them as uncertain evidences into this Bayesian network to perform posterior inference.

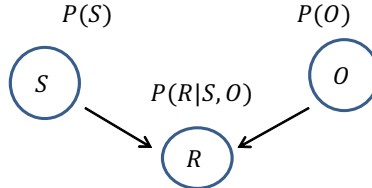


Figure 3: Within-triplet Bayesian network where prior probabilities of subject and object are combined with conditional probability of relationship.

4.2 Uncertain evidence

We denote any trained SGG model with parameter θ_m which generates measurement probabilities of subject, object, and relationship of every triplet for an image I as $P_{\theta_m, I}(S)$, $P_{\theta_m, I}(O)$, and $P_{\theta_m, I}(R)$. We consider these measurements as uncertain evidences of the nodes in the within-triplet BN in Figure 3. Since these evidences are uncertain, we incorporate them as virtual evidences into the BN as shown in Figure 4. Following the virtual evidence method proposed by Judea Pearl in [20], we introduce binary virtual evidence nodes Z_s , Z_o , and Z_r as children of their respective

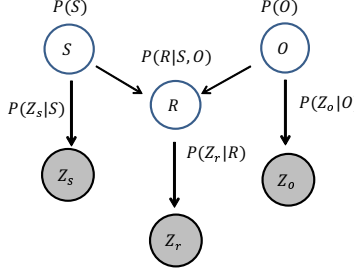


Figure 4: Uncertain evidence of each entity of triplet is incorporated into the Bayesian network as conditional probability of virtual evidence node denoted as Z_s , Z_o , and Z_r .

parent evidence nodes S , R , and O . According to Theorem 5 in [1], the conditional distribution of these virtual nodes maintain the following likelihood ratios

$$\begin{aligned} P(Z_s = 1|s_1) : \dots : P(Z_s = 1|s_n) &= \frac{P_{I,\theta_m}(s_1)}{P(s_1)} : \dots : \frac{P_{I,\theta_m}(s_n)}{P(s_n)} \\ P(Z_o = 1|o_1) : \dots : P(Z_o = 1|o_n) &= \frac{P_{I,\theta_m}(o_1)}{P(o_1)} : \dots : \frac{P_{I,\theta_m}(o_n)}{P(o_n)} \\ P(Z_r = 1|r_1) : \dots : P(Z_r = 1|r_n) &= \frac{P_{I,\theta_m}(r_1)}{P(r_1)} : \dots : \frac{P_{I,\theta_m}(r_n)}{P(r_n)} \end{aligned} \quad (3)$$

where $P(S = s)$, $P(O = o)$, and $P(R = r)$ are the marginal probabilities of subject, object, and relationship node and $P_{\theta_m,I}(S)$, $P_{\theta_m,I}(O)$, and $P_{\theta_m,I}(R)$ are their observed measurement probabilities from image I with model θ_m . Now, we have a complete Bayesian network in Figure 4 with well-defined marginal and conditional probabilities. A brief discussion on uncertain evidence and their incorporation in Bayesian network is discussed in the supplementary material.

4.3 Within-Triplet Inference (WTI) of triplets

After the evidence incorporation as virtual evidences, the posterior joint distribution of triplet nodes becomes

$$\begin{aligned} P(S = s, R = r, O = o | Z_s = 1, Z_o = 1, Z_r = 1) \\ \propto P(Z_s = 1|s)P(s)P(Z_o = 1|o)P(o)P(Z_r = 1|r)P(r|s, o) \\ \propto P_{I,\theta_m}(S = s)P_{I,\theta_m}(O = o) \frac{P_{I,\theta_m}(R = r)}{P(R = r)} P(r|s, o) \end{aligned} \quad (4)$$

The Maximum a-Posterior (MAP) of this posterior joint distribution becomes

$$\begin{aligned} s^*, r^*, o^* &= \arg \max_{S,R,O} P(S, R, O | Z_s = 1, Z_o = 1, Z_r = 1) \\ &= \arg \max_{S,R,O} P_{I,\theta_m}(S)P_{I,\theta_m}(O) \frac{P_{I,\theta_m}(R)}{P(R)} P(R|S, O) \end{aligned} \quad (5)$$

In Eqn. (5), the within-triplet dependency of relationship is encoded in $P(R|S, O)$ and the measurement probability of relationship $P_{I,\theta_m}(R)$ is debiased by its marginal probability $P(R)$. The subject and object uncertainties are encoded in $P_{I,\theta_m}(S)$ and $P_{I,\theta_m}(O)$. We include some special cases of the MAP Eqn. (5) in the supplementary material.

4.4 Constraint optimization in inferred triplets

Any object entity E_i can reside in multiple triplets as subject S or object O and after individual triplet inference, their inferred values can be different in different triplets. However, to form a valid scene graph, their values should be same after the inference. Formally, if object entity E_i resides in J triplets, their inferred values E_{ij}^* must follow the following constraint

$$E_{i1}^* = E_{i2}^* = \dots = E_{ij}^* = \dots = E_{iJ}^* = E_i^I \quad (6)$$

One of the most straightforward ways to satisfy such constraint would be to take the mode of these inferred values as the final value for E_i . However, any object entity E_i^* should be consistent with respect to all of its connected triplets, and hence we formulate a two-step optimization algorithm to infer E_i^* and R_i^* from their connections.

Object Updating: In the first step, we infer each object label E_i^* combining its measurement probability $P_{I,\theta_m}(E_i)$ with the within-triplet probabilities of its connected triplets. We denote T_i^S and T_i^O as the sets of triplets where E_i acts as subject and object respectively

$$\begin{aligned} T_i^S &= \{t_p : t_p(S) = E_i\} \\ T_i^O &= \{t_q : t_q(O) = E_i\} \end{aligned} \quad (7)$$

The updated object probability for object E_i is derived as

$$\begin{aligned} f(E_i) &= P_{I,\theta_m}(E_i) \left(\sum_{t_p \in T_i^S} P(R = r_{t_p}^I | S = E_i, O = o_{t_p}^I) \right. \\ &\quad \left. + \sum_{t_q \in T_i^O} P(R = r_{t_q}^I | S = s_{t_q}^I, O = E_i) \right) \end{aligned} \quad (8)$$

Intuitively speaking, the updated object probability $f(E_i)$ derived in Eqn. (8) combines the uncertain evidence of an object entity $P_{I,\theta_m}(E_i)$ with the prior probabilities of the within-triplet Bayesian networks of all of its connected triplet. We infer E_i^* by

$$E_i^* = \arg \max f(E_i) \quad (9)$$

Relationship Updating: After the first step is completed for each object entities, the conflicts of object entities are resolved with updated entity values. In the second step, we update the relationship label of each triplet based on the updated subject and object values

$$\begin{aligned} R_j^* &= \arg \max_R P(R_j | Z_r = 1, S = s_j, O = O_j) \\ &= \arg \max_R \frac{P_{I,\theta_m}(R_j)}{P(R_j)} P(R_j | S = s_j, O = o_j) \end{aligned} \quad (10)$$

The detailed derivation and pseudo-code is provided in supplementary material. We denote this as *constraint optimization* in our overview in Figure 2.

5 Learning BN with embedding similarity

The within-triplet priors $P(S) \in \mathbb{R}^{N_s}$, $P(O) \in \mathbb{R}^{N_o}$, and conditional distribution $P(R|S, O) \in \mathbb{R}^{N_s \times N_o \times N_r}$ are learnt from annotations of training data where N_s , N_o , and N_r denote the number of categories of subject, object, and relationship. A training dataset of $\mathbb{Z}^{3 \times N}$ is created by collecting all ground truth (GT) triplets in the training images where N is the total number of training triplets. Using this training dataset, we apply MLE to estimate the parameters of the Bayesian network. The MLE estimation of $P(R|S, O)$ and $P(R)$ can be written as

$$\begin{aligned} P(R = r | S = s, O = o) &= \frac{N_{s,r,o}^c}{\sum_{r'} N_{s,r',o}^c} \\ P(R) &= \sum_{S,O} P(R|S,O)P(S)P(O) \end{aligned} \quad (11)$$

where $N_{s,r,o}^c$ is the count of triplet with $S = s, O = o$ and $R = r$. However, because of selecting only top N_r relationships from the training data, many semantically similar triplets whose relationships lie outside these top N_r , are ignored in this count (e.g. ‘man consuming pizza’ is ignored whereas ‘man eating pizza’ is considered as valid triplet). Hence, we propose a novel sample augmentation method using off-the-shelf sentence embedding models [30] where all the ignored invalid triplets, lying within a ϵ -neighbourhood of a valid triplet in the embedding space, are counted as augmented samples of that valid triplet. For any subject and object pair with $S = s, O = o$, we denote any valid triplet as $T = \{s, r, o\}$ and invalid triplet as $T_i = \{s, r_i, o\}$ where $r \in N_r$ and $r_i \notin N_r$. Now, if we denote the original count of T as $N_{s,r,o}^c$ and that of T_i as $N_{s,r_i,o}$, we can augment the original count as following

$$N_{s,r,o}^a = \begin{cases} N_{s,r,o}^c + \sum_{T_i \in \mathcal{N}_\epsilon(T)} N_{s,r_i,o} & \text{if } \mathcal{N}_\epsilon(T) \neq \emptyset \\ N_{s,r,o}^c & \text{if } \mathcal{N}_\epsilon(T) = \emptyset \end{cases} \quad (12)$$

DS	Method	Recall and Mean Recall @K					
		PredCls		SGCls		SGDet	
		R@50/100	mR@50/100	R@50/100	mR@50/100	R@50/100	mR@50/100
VG	IMP [◦] [32]	61.63/ 63.63	11.53/ 12.38	36.14/ 37.09	5.69/ 5.98	28.04/ 31.30	4.89/ 5.84
	Inf-IMP	59.93/ 62.02	25.14/ 28.34	36.02/ 37.09	12.57/ 14.06	26.50/ 29.51	8.58/ 10.67
	MOTIF [◦] [42]	59.57/ 63.95	12.88/ 15.47	36.45/ 38.47	7.66/ 8.83	26.85/ 30.50	5.61/ 6.73
	Inf-MOTIF	51.49/ 55.07	24.67/ 30.71	32.15/ 33.79	14.50/ 17.40	23.94/ 27.09	9.36/ 11.71
	VCTree [◦] [27]	65.46/ 67.18	15.36/ 16.61	44.15/ 45.11	9.17/ 9.83	29.94/ 32.57	6.21/ 6.96
	Inf-VCTree	59.50/ 60.97	28.14/ 30.72	40.69/ 41.55	17.31/ 19.40	27.74/ 30.10	10.40/ 11.86
	Unb-MOTIF [◦] [26]	45.87/ 51.24	24.75/ 28.69	26.30/ 28.78	13.21/ 15.06	16.25/ 19.53	8.65/ 10.47
	Inf-Unb-MOTIF	42.40/ 46.82	28.64/ 35.65	24.13/ 26.28	15.85/ 18.88	15.06/ 18.03	9.60/ 11.94
	DLFE-MOTIF [◦] [3]	51.63/ 53.28	26.87/ 28.75	28.79/ 29.66	15.61/ 16.38	24.22/ 27.95	10.62/ 12.61
	Inf-DLFE-MOTIF	43.27/ 44.82	35.25/ 38.20	24.34/ 25.14	19.74/ 20.66	20.61/ 23.80	14.07/ 16.76
GQA	BGNN [◦] [14]	58.15/ 60.41	29.46/ 31.83	-/-	-/-	30.26/ 34.98	10.37/ 12.31
	Inf-BGNN	55.42/ 57.47	32.18/ 34.27	-/-	-/-	26.16/ 30.11	13.24/ 16.10
	IMP [◦] [32]	61.94/ 63.68	13.04/ 13.74	34.25/ 34.83	7.46/ 7.80	25.39/ 27.42	5.77/ 6.58
	Inf-IMP	61.87/ 63.98	35.14/ 37.54	33.19/ 34.01	19.06/ 20.33	23.46/ 25.56	12.17/ 14.13
	MOTIF [◦] [42]	68.29/ 69.65	20.67/ 21.56	34.89/ 35.43	10.90/ 11.31	27.83/ 29.38	7.38/ 8.32
	Inf-MOTIF	62.95/ 64.23	37.93/ 40.07	31.82/ 32.35	19.09/ 20.00	25.51/ 26.86	14.34/ 15.84
	VCTree [◦] [27]	68.83/ 70.14	22.07/ 23.01	35.04/ 35.58	10.59/ 10.97	27.21/ 28.79	7.03/ 7.75
	Inf-VCTree	62.80/ 64.05	39.44/ 41.63	32.23/ 32.80	19.18/ 20.03	25.04/ 26.44	13.58/ 15.11
	Unb-MOTIF [◦] [26]	51.87/ 55.87	27.81/ 32.30	26.10/ 28.06	14.09/ 16.33	18.22/ 21.63	10.78/ 12.89
	Inf-Unb-MOTIF	49.86/ 53.60	34.45/ 40.80	24.76/ 26.74	17.18/ 20.59	16.84/ 19.94	12.35/ 14.76

Table 1: R@K and mR@K results of inference with prefix ‘Inf-’. We observe a significant increase in **mR@K** with a slight decrease in **R@K** for all baseline models in both dataset. Graph constraint is applied in all setting.

Here, ϵ is a hyper-parameter and $\mathcal{N}_\epsilon(T)$ is defined as the ϵ -neighbourhood of a valid triplet T in the embedding space using the following criteria

$$\mathcal{N}_\epsilon(T) = \{T_i : \phi(f(T), f(T_i)) < \epsilon\} \quad (13)$$

where $\phi(f(T_a), f(T_b))$ represents the distance between two embedding vectors of two triplet $f(T_a)$ and $f(T_b)$. Since the embeddings lie on unit-sphere, we employ cosine similarity to measure the angular distance between two embedding vectors of two triplets. We visualize the ϵ -neighbourhood of a valid triplet T in Figure 5.

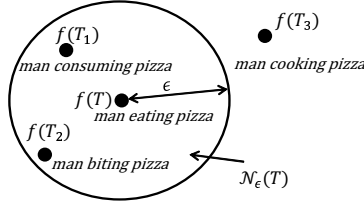


Figure 5: $\mathcal{N}_\epsilon(T)$ in the embedding space where $f(T_1), f(T_2) \in \mathcal{N}_\epsilon(T)$ and $f(T_3) \notin \mathcal{N}_\epsilon(T)$.

6 Experimental settings

6.1 Dataset

We evaluate our proposed method on two datasets: (1) Visual Genome (**VG**), and (2) **GQA**.

(1) Visual Genome: For SGG, the most commonly used database is the Visual Genome (**VG**) [11] and from the original database, the most frequent 150 object and 50 predicate categories are retained [32, 42]. We adopt the standard train-test split ratio of 70 : 30. The number of prior triplets from original training dataset is around 323K and after augmenting with $\epsilon = 0.05$, the number rises to around 391K.

(2) GQA: GQA [8] is a refined dataset derived from the VG images. We retain images only with the most frequent 150 object and 50 relationship categories. We train on around $50k$ valid images and perform evaluation on the validation dataset of valid $7k$ images. We collect over $190K$ prior triplets and after embedding-based augmentation with $\epsilon = 0.05$, the number rises to around $200K$.

6.2 Task description

A triplet is considered correct if the subject, relationship, and object label matches with the ground truth labels and the boundary boxes of subject and object has Intersection over Union (IoU) of at least 50% with the ground truth annotations. We consider three test-time tasks, defined by [32], - (1) PredCls: known object labels and locations, (2) SGCl: known object locations, and (3) SGDet: where no information about objects are known. We apply graph constraint for all the tasks where for each pair of the objects, only one relationship is allowed.

6.3 Evaluation metrics

The performance of our debiased SGGs is evaluated through recall (**R@K**) and mean recall (**mR@K**). **R@K** of an image is computed as fraction of ground truth triplets in top@K predicted triplets [19] whereas **mR@K** computes recall for each relationship separately and then the average over all relationships are computed [2, 27].

6.4 Implementation details

We perform training and testing of the baseline models released by [26], [3], and [14]. We collect measurement results and ground truth annotations of the testing database using Python. For sample augmentation, we employ sentence transformers in Python and from the original and augmented annotations, we learn the within-triplet prior and perform posterior inference in MATLAB on a computer with core i5 7th generation Intel processor running at 2.5 MHz with 8.00 GB RAM. The total training time for the prior probabilities of **VG** dataset is 968s and that of **GQA** is 430s. The inference task per image requires 0.13s.

7 Experimental results

7.1 Quantitative results

We generate triplet measurements from four classical SGG models - (1) IMP [32], (2) MOTIF [42], (3) VCTree [27], and (4) Unb-MOTIF [26] from codebase [26] (\diamond), and two recent-most SOTA SGG models released by (1) DLFE-MOTIF [3] and (2) BGNN [14] (\diamond). Considering these measurements as the uncertain evidences, we first perform within-triplet inference and then conduct two-step updating. We denote the final results with prefix ‘Inf-’. The Bayesian network is learnt from the augmented counts of triplet derived by Eqn. (12). We report **R@K** and **mR@K** for all three tasks with **VG** and **GQA** in Table 1. We also include a separate comparison with other bias removal techniques (1) **Unb-** [26], (2) **DLFE-** [3], and (3) **NICE-[12]** in Table 2. Our method performs better in balancing the *head* and *tail* classes without any retraining of the biased model.

Method	Re-train	R@K		mR@K
		@50/100	@50/100	
VCTree[27]	-	65.5/ 67.2	15.4/ 16.6	
Unb-VCTree [26]	No	47.2/ 51.6	25.4/ 28.7	
DLFE-VCTree [3]	Yes	51.8/ 53.5	25.3/ 27.1	
NICE-VCTree [12]	Yes	55.0/ 56.9	30.7/ 33.0	
Inf-VCTree (Ours)	No	59.5/ 61.0	28.1/ 30.7	

Table 2: Comparison with other de-biasing methods in PredCls. Without re-training, our loss in **R@K** is significantly lower and gain in **mR@K** is higher or competitive than other SOTA debiasing methods.

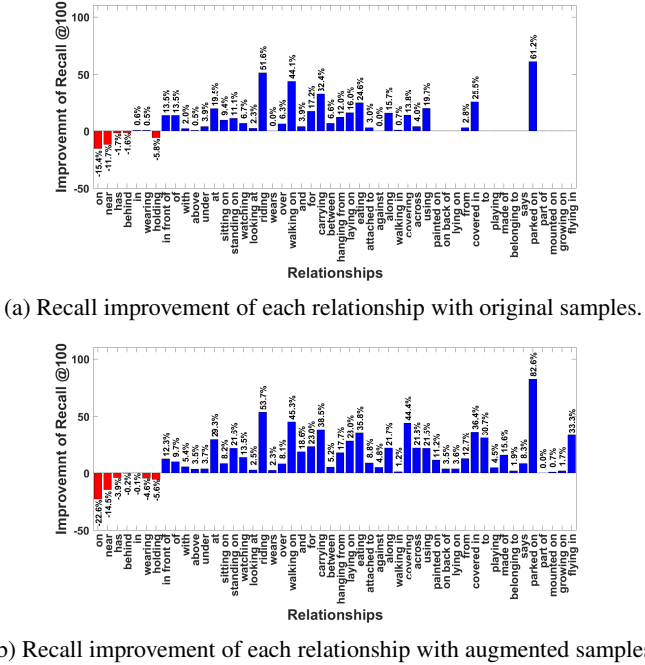
Method	R@K	Mean R@K
	@50/100	@50/100
Uncertain evidence (VCTree)	65.5/ 67.2	15.4/ 16.6
WT BN only (org) (FREQ)	64.3/ 65.8	16.1/ 17.5
WT BN only (aug) (Ours)	62.7/ 64.2	16.3/ 17.8
WT BN (org) + Unc. Evi (Ours)	62.5/ 64.1	22.7/ 24.8
WT BN (aug) + Unc. Evi (Ours)	59.5/ 61.0	28.1/ 30.7

Table 3: Ablation study on PredCls performance for VG. We observe consistent improvement of **mR@K** starting with uncertain evidences and ending in posterior inference with uncertain evidence with BN learnt from augmented samples.

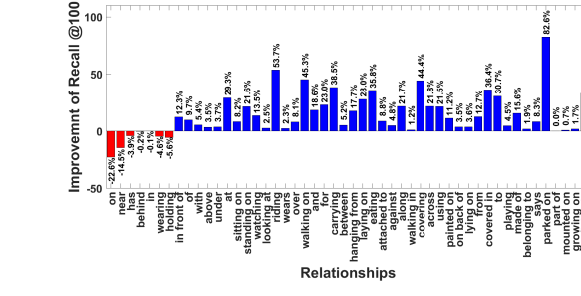
7.2 Analysis

7.2.1 Visualization of mean recall improvement

We visualize the improvement of tail classes with BN learnt from original and augmented samples in Figure 6a and 6b.



(a) Recall improvement of each relationship with original samples.



(b) Recall improvement of each relationship with augmented samples.

Figure 6: Improvement of mean recalls with VCTree [27] evidences for PredCls task in VG. Relationships are ordered in descending order of their frequencies. Our proposed BN learnt with original improves the *mid* relationships whereas the embedding based augmentation improves both the *mid* and the *tail* ones. In both cases, the *head* relationships are worsened after debiasing.

7.2.2 Ablation study on prior and uncertain evidence

We perform ablation study on the measurement results of PredCls task by VCTree [27] in Table 3.

7.2.3 Ablation study on conflict resolution

We observe the effectiveness of the constrained optimization over mode version in Table 4.

Method	R@K	mR@K
	@50/100	@50/100
VCTree [27]	44.2/ 45.1	9.2/ 9.8
Inf-VCTree (Conflict res. by mode)	40.3/ 41.2	16.9/ 18.7
Inf-VCTree (Conflict res. by opt.)	40.7/ 41.6	17.3/ 19.4

Table 4: Ablation study on conflict resolution for VCTree SGCLs performance for Visual Genome.

7.2.4 Effect of ϵ on training data augmentation

We observe the effect of ϵ on recall performances in Table 5 with VCTree baseline [27].

Method	ϵ	Recall@K	Mean Recal@K
		@50/@100	@50/@100
Inf- VCTree (org)	-	62.48/ 64.06	22.74/ 24.78
Inf- VCTree (aug)	0.03	59.44/ 60.88	28.01/ 30.55
	0.05	59.50/ 60.97	28.14/ 30.72
	0.07	59.27/ 60.73	28.28/ 30.92

Table 5: Effect of ϵ on PredCls performance for VG. We find that using larger ϵ tends to hurt the majority classes more. Based on this study, we choose $\epsilon = 0.05$ for our final experiments.

7.2.5 Effect on zero-shot recall

The zero-shot prediction of measurement model is compromised after posterior inference due to MLE-based learning of BN. However, since unseen triplets will have higher entropy than the seen ones in the prediction phase, we can filter out the high entropy triplets so that they do not get refined by the BN. An ablation study with respect to entropy threshold is shown in Table 6.

Method	Entropy Th.	ZS R@100	Mean R@100
		org/aug	org/aug
VCTree [27]	-	6.02	16.61
Inf-VCTree	0	6.02/6.02	16.61/16.61
	1.5	5.81/6.13	20.20/22.71
	2.5	5.47/6.03	24.42/29.28
	3.912	1.06/2.30	24.78/30.70

Table 6: Zero-shot recall on PredCls for VG for VCTree. Lower entropy thresholds restore the zero-shot capability of measurement models by hurting the mean recall. We choose not to use any threshold (last row) to maximize performance in mean recall.

8 Limitations

While improving **mR@K** by our proposed method, we lose performance in **R@K**. This phenomenon is prevailing in SGG debiasing works since we are perturbing the ‘head’ classes to gain improvement in the ‘tail’. Moreover, the augmentation hyper-parameter ϵ may vary from dataset to dataset and need to be chosen carefully. Another weakness is the compromise in zero-shot prediction capability of a measurement model due to MLE based learning of BN.

9 Conclusion

We proposed a debiasing strategy of scene graphs which combines prior knowledge and uncertain evidences of triplets in Bayesian framework. We performed within-triplet MAP inference to ensure the within-triplet dependency of a relationship and we optimally solved the conflicts of object entities in different triplets. We augmented the count of valid triplets with semantically similar invalid triplets to alleviate sample insufficiency. Our method showcased significant improvement of mean recall with baseline measurements. We also attained a better balance between majority and minority performances of the relationships. In future, we will extend the MAP inference for multiply connected triplets and we will explore well-defined criteria for zero-shot refinement to restore the zero-shot recall of the measurement models.

References

- [1] Hei Chan and Adnan Darwiche. On the revision of probabilistic beliefs using uncertain evidence. *Artificial Intelligence*, 163(1):67–90, 2005.
- [2] Tianshui Chen, Weihao Yu, Riquan Chen, and Liang Lin. Knowledge-embedded routing network for scene graph generation. In *Proceedings of the IEEE Conference on Computer Vision and Pattern Recognition*, pages 6163–6171, 2019.
- [3] Meng-Jiun Chiou, Henghui Ding, Hanshu Yan, Changhu Wang, Roger Zimmermann, and Jiashi Feng. Recovering the unbiased scene graphs from the biased ones. In *Proceedings of the 29th ACM International Conference on Multimedia*, pages 1581–1590, 2021.
- [4] Bo Dai, Yuqi Zhang, and Dahua Lin. Detecting visual relationships with deep relational networks. In *Proceedings of the IEEE conference on computer vision and Pattern recognition*, pages 3076–3086, 2017.
- [5] Alakh Desai, Tz-Ying Wu, Subarna Tripathi, and Nuno Vasconcelos. Learning of visual relations: The devil is in the tails. In *Proceedings of the IEEE/CVF International Conference on Computer Vision*, pages 15404–15413, 2021.
- [6] Jiuxiang Gu, Handong Zhao, Zhe Lin, Sheng Li, Jianfei Cai, and Mingyang Ling. Scene graph generation with external knowledge and image reconstruction. In *Proceedings of the IEEE Conference on Computer Vision and Pattern Recognition*, pages 1969–1978, 2019.
- [7] Yuyu Guo, Lianli Gao, Xuanhan Wang, Yuxuan Hu, Xing Xu, Xu Lu, Heng Tao Shen, and Jingkuan Song. From general to specific: Informative scene graph generation via balance adjustment. In *Proceedings of the IEEE/CVF International Conference on Computer Vision*, pages 16383–16392, 2021.
- [8] Drew A Hudson and Christopher D Manning. Gqa: A new dataset for real-world visual reasoning and compositional question answering. In *Proceedings of the IEEE/CVF Conference on Computer Vision and Pattern Recognition*, pages 6700–6709, 2019.
- [9] Zih-Siou Hung, Arun Mallya, and Svetlana Lazebnik. Contextual translation embedding for visual relationship detection and scene graph generation. *IEEE transactions on pattern analysis and machine intelligence*, 43(11):3820–3832, 2020.
- [10] Justin Johnson, Agrim Gupta, and Li Fei-Fei. Image generation from scene graphs. In *Proceedings of the IEEE conference on computer vision and pattern recognition*, pages 1219–1228, 2018.
- [11] Ranjay Krishna, Yuke Zhu, Oliver Groth, Justin Johnson, Kenji Hata, Joshua Kravitz, Stephanie Chen, Yannis Kalantidis, Li-Jia Li, David A Shamma, et al. Visual genome: Connecting language and vision using crowdsourced dense image annotations. *International Journal of Computer Vision*, 123(1):32–73, 2017.
- [12] Lin Li, Long Chen, Yifeng Huang, Zhimeng Zhang, Songyang Zhang, and Jun Xiao. The devil is in the labels: Noisy label correction for robust scene graph generation. In *Proceedings of the IEEE/CVF Conference on Computer Vision and Pattern Recognition (CVPR)*, pages 18869–18878, June 2022.
- [13] Rongjie Li, Songyang Zhang, and Xuming He. Sgtr: End-to-end scene graph generation with transformer. In *Proceedings of the IEEE/CVF Conference on Computer Vision and Pattern Recognition (CVPR)*, pages 19486–19496, June 2022.
- [14] Rongjie Li, Songyang Zhang, Bo Wan, and Xuming He. Bipartite graph network with adaptive message passing for unbiased scene graph generation. In *Proceedings of the IEEE/CVF Conference on Computer Vision and Pattern Recognition*, pages 11109–11119, 2021.
- [15] Wei Li, Haiwei Zhang, Qijie Bai, Guoqing Zhao, Ning Jiang, and Xiaojie Yuan. Pndl: Predicate probability distribution based loss for unbiased scene graph generation. In *Proceedings of the IEEE/CVF Conference on Computer Vision and Pattern Recognition (CVPR)*, pages 19447–19456, June 2022.
- [16] Xiaodan Liang, Lisa Lee, and Eric P Xing. Deep variation-structured reinforcement learning for visual relationship and attribute detection. In *Proceedings of the IEEE conference on computer vision and pattern recognition*, pages 848–857, 2017.
- [17] Xin Lin, Changxing Ding, Jinquan Zeng, and Dacheng Tao. Gps-net: Graph property sensing network for scene graph generation. In *Proceedings of the IEEE/CVF Conference on Computer Vision and Pattern Recognition*,

pages 3746–3753, 2020.

[18] Hugo Liu and Push Singh. Conceptnet—a practical commonsense reasoning tool-kit. *BT technology journal*, 22(4):211–226, 2004.

[19] Cewu Lu, Ranjay Krishna, Michael Bernstein, and Li Fei-Fei. Visual relationship detection with language priors. In *European conference on computer vision*, pages 852–869. Springer, 2016.

[20] Judea Pearl. *Probabilistic reasoning in intelligent systems: networks of plausible inference*. Elsevier, 2014.

[21] Julia Peyre, Ivan Laptev, Cordelia Schmid, and Josef Sivic. Detecting unseen visual relations using analogies. In *Proceedings of the IEEE/CVF International Conference on Computer Vision*, pages 1981–1990, 2019.

[22] Brigit Schroeder, Subarna Tripathi, and Hanlin Tang. Triplet-aware scene graph embeddings. In *Proceedings of the IEEE/CVF International Conference on Computer Vision Workshops*, pages 0–0, 2019.

[23] Sahand Sharifzadeh, Sina Moayed Baharlou, and Volker Tresp. Classification by attention: Scene graph classification with prior knowledge. *arXiv preprint arXiv:2011.10084*, 2020.

[24] Jiaxin Shi, Hanwang Zhang, and Juanzi Li. Explainable and explicit visual reasoning over scene graphs. In *Proceedings of the IEEE/CVF Conference on Computer Vision and Pattern Recognition*, pages 8376–8384, 2019.

[25] Mohammed Suhail, Abhay Mittal, Behjat Siddique, Chris Broaddus, Jayan Eledath, Gerard Medioni, and Leonid Sigal. Energy-based learning for scene graph generation. In *Proceedings of the IEEE/CVF Conference on Computer Vision and Pattern Recognition*, pages 13936–13945, 2021.

[26] Kaihua Tang, Yulei Niu, Jianqiang Huang, Jiaxin Shi, and Hanwang Zhang. Unbiased scene graph generation from biased training. In *Proceedings of the IEEE/CVF Conference on Computer Vision and Pattern Recognition*, pages 3716–3725, 2020.

[27] Kaihua Tang, Hanwang Zhang, Baoyuan Wu, Wenhan Luo, and Wei Liu. Learning to compose dynamic tree structures for visual contexts. In *Proceedings of the IEEE/CVF Conference on Computer Vision and Pattern Recognition*, pages 6619–6628, 2019.

[28] Antonio Torralba and Alexei A Efros. Unbiased look at dataset bias. In *CVPR 2011*, pages 1521–1528. IEEE, 2011.

[29] Hai Wan, Yonghao Luo, Bo Peng, and Wei-Shi Zheng. Representation learning for scene graph completion via jointly structural and visual embedding. In *IJCAI*, pages 949–956. Stockholm, Sweden, 2018.

[30] Thomas Wolf, Lysandre Debut, Victor Sanh, Julien Chaumond, Clement Delangue, Anthony Moi, Pierric Cistac, Tim Rault, Rémi Louf, Morgan Funtowicz, Joe Davison, Sam Shleifer, Patrick von Platen, Clara Ma, Yacine Jernite, Julien Plu, Canwen Xu, Teven Le Scao, Sylvain Gugger, Mariama Drame, Quentin Lhoest, and Alexander M. Rush. Transformers: State-of-the-art natural language processing. In *Proceedings of the 2020 Conference on Empirical Methods in Natural Language Processing: System Demonstrations*, pages 38–45, Online, Oct. 2020. Association for Computational Linguistics.

[31] Sanghyun Woo, Dahun Kim, Donghyeon Cho, and In So Kweon. Linknet: Relational embedding for scene graph. *arXiv preprint arXiv:1811.06410*, 2018.

[32] Danfei Xu, Yuke Zhu, Christopher B Choy, and Li Fei-Fei. Scene graph generation by iterative message passing. In *Proceedings of the IEEE conference on computer vision and pattern recognition*, pages 5410–5419, 2017.

[33] Minghao Xu, Meng Qu, Bingbing Ni, and Jian Tang. Joint modeling of visual objects and relations for scene graph generation. *Advances in Neural Information Processing Systems*, 34, 2021.

[34] Gengcong Yang, Jingyi Zhang, Yong Zhang, Baoyuan Wu, and Yujiu Yang. Probabilistic modeling of semantic ambiguity for scene graph generation. In *Proceedings of the IEEE/CVF Conference on Computer Vision and Pattern Recognition*, pages 12527–12536, 2021.

[35] Jianwei Yang, Jiasen Lu, Stefan Lee, Dhruv Batra, and Devi Parikh. Graph r-cnn for scene graph generation. In *Proceedings of the European conference on computer vision (ECCV)*, pages 670–685, 2018.

[36] Xu Yang, Kaihua Tang, Hanwang Zhang, and Jianfei Cai. Auto-encoding scene graphs for image captioning. In *Proceedings of the IEEE/CVF Conference on Computer Vision and Pattern Recognition*, pages 10685–10694, 2019.

[37] Yuan Yao, Ao Zhang, Xu Han, Mengdi Li, Cornelius Weber, Zhiyuan Liu, Stefan Wermter, and Maosong Sun. Visual distant supervision for scene graph generation. *arXiv preprint arXiv:2103.15365*, 2021.

[38] Keren Ye and Adriana Kovashka. Linguistic structures as weak supervision for visual scene graph generation. In *Proceedings of the IEEE/CVF Conference on Computer Vision and Pattern Recognition*, pages 8289–8299, 2021.

[39] Ruichi Yu, Ang Li, Vlad I Morariu, and Larry S Davis. Visual relationship detection with internal and external linguistic knowledge distillation. In *Proceedings of the IEEE international conference on computer vision*, pages 1974–1982, 2017.

[40] Alireza Zareian, Svebor Karaman, and Shih-Fu Chang. Bridging knowledge graphs to generate scene graphs. In *European Conference on Computer Vision*, pages 606–623. Springer, 2020.

[41] Alireza Zareian, Zhecan Wang, Haoxuan You, and Shih-Fu Chang. Learning visual commonsense for robust scene graph generation. In *Computer Vision–ECCV 2020: 16th European Conference, Glasgow, UK, August 23–28, 2020, Proceedings, Part XXIII 16*, pages 642–657. Springer, 2020.

[42] Rowan Zellers, Mark Yatskar, Sam Thomson, and Yejin Choi. Neural motifs: Scene graph parsing with global context. *arXiv:1711.06640*, 2017.

[43] Hanwang Zhang, Zawlin Kyaw, Shih-Fu Chang, and Tat-Seng Chua. Visual translation embedding network for visual relation detection. In *Proceedings of the IEEE conference on computer vision and pattern recognition*, pages 5532–5540, 2017.

[44] Ji Zhang, Kevin J Shih, Ahmed Elgammal, Andrew Tao, and Bryan Catanzaro. Graphical contrastive losses for scene graph parsing. In *Proceedings of the IEEE/CVF Conference on Computer Vision and Pattern Recognition*, pages 11535–11543, 2019.

[45] Yi Zhou, Shuyang Sun, Chao Zhang, Yikang Li, and Wanli Ouyang. Exploring the hierarchy in relation labels for scene graph generation. *arXiv preprint arXiv:2009.05834*, 2020.

A Special cases of MAP inference

In this section, we describe some special cases of MAP inference in Eqn. (7).

1. **FREQ baseline [42], subject and object is known:** In this scenario, we want to predict the relationship label of a triplet only from its known subject ($S = S_g$) and object label ($O = O_g$). Hence, we can write

$$\begin{aligned} P_{I,\theta_m}(S) &= \mathbb{1}_{\{S=S_g\}} \\ P_{I,\theta_m}(O) &= \mathbb{1}_{\{O=O_g\}} \end{aligned} \quad (14)$$

Since there is no image measurement for the relationship label, the MAP Eqn. (7) becomes

$$\begin{aligned} R^* &= \arg \max_R P(R|S = S_g, O = O_g) \\ &= \arg \max_R P(R|S_g, O_g) \end{aligned} \quad (15)$$

This is essentially the FREQ baseline proposed by [42]

2. **Synthetic relationship, subject and object is known:** The within-triplet Bayesian network is a generative model for subject, object, and relationship. Hence, we can generate synthetic samples of relationship R_{syn} given subject and object as following

$$R_{syn} \sim P(R|S_g, O_g) \quad (16)$$

3. **Uncertain evidence for relationship, subject and object is known:** In presence of the uncertainty associated only with the relationship label from measurement model θ_m , the MAP decision becomes

$$\begin{aligned} R^* &= \arg \max_R P(R|Z_r = 1, S = S_g, O = O_g) \\ &= \arg \max_R \frac{P_{I,\theta_m}(R)}{P(R)} P(R|S_g, O_g) \end{aligned} \quad (17)$$

This is essentially the PREDCIs setting [32], where we infer the relationship given that categories and bounding boxes of subject and object of a triplet.

4. **No Bayesian network, only evidence uncertainties:** In this case, we infer each component of a triplet independently from its measurement uncertainty. Hence, the MAP decision becomes as following

$$\begin{aligned} S^* &= \arg \max_S P_{I,\theta_m}(S) \\ O^* &= \arg \max_O P_{I,\theta_m}(O) \\ R^* &= \arg \max_R P_{I,\theta_m}(R) \end{aligned} \quad (18)$$

This is essentially predicting the labels of a triplet from the probabilities that the classification head of the SOTA deep-learning based methods produce.

From the discussion above, we can conclude that the MAP inference in Eqn. (7) is the most general framework and all the other cases can be considered a special case of that MAP inference.

B Constrained Optimization for Conflict Resolution

Any object entity E_i can reside as subjects or objects in multiple triplets. We denote T_i^S as the set of triplets where E_i acts as subject and T_i^O as the set of triplets where E_i acts as object. We formally define them as following

$$\begin{aligned} T_i^S &= \{t_p : t_p(S) = E_i\} \\ T_i^O &= \{t_q : t_q(O) = E_i\} \end{aligned} \quad (19)$$

Now, we can define an optimization function by summing up all the posterior probabilities of within-triplet Bayesian network from all triplets in T_S and in T_O as following

$$\begin{aligned} f = \sum_{t_p \in T_i^S} P(S_{t_p}, R_{t_p}, O_{t_p} | Z_{S_{t_p}} = 1, Z_{R_{t_p}} = 1, Z_{O_{t_p}} = 1) + \\ \sum_{t_q \in T_i^O} P(S_{t_q}, R_{t_q}, O_{t_q} | Z_{S_{t_q}} = 1, Z_{R_{t_q}} = 1, Z_{O_{t_q}} = 1) \end{aligned} \quad (20)$$

Evaluating this optimization function for every possible combination of subject, relationships and object in multiple connected triplets is computationally challenging and hence we propose a two-step alternating approach. In the first step, for each entity, we modify the measurement probabilities of all nodes connected to object entity E_i according to the inferred values. In this way, we essentially reduce all the evidence uncertainty and only keep the uncertainty to object entity E_i . The modification can be written as following

$$\begin{aligned} P_{I,\theta_m}(S_{t_p}) &= P_{I,\theta_m}(E_i) \\ P_{I,\theta_m}(R_{t_p}) &= \mathbb{1}_{\{R_{t_p} = r_{t_p}^I\}}, \quad \forall t_p \in T_i^S \\ P_{I,\theta_m}(O_{t_p}) &= \mathbb{1}_{\{O_{t_p} = o_{t_p}^I\}}, \quad \forall t_p \in T_i^S \\ P_{I,\theta_m}(S_{t_q}) &= \mathbb{1}_{\{S_{t_q} = s_{t_q}^I\}}, \quad \forall t_q \in T_i^O \\ P_{I,\theta_m}(R_{t_q}) &= \mathbb{1}_{\{R_{t_q} = r_{t_q}^I\}}, \quad \forall t_q \in T_i^O \\ P_{I,\theta_m}(O_{t_q}) &= P_{I,\theta_m}(E_i) \end{aligned} \quad (21)$$

Now, plugging these modified uncertain evidences into Eqn. 20 and using MAP Eqn. 5, we can simplify the objective function by

$$\begin{aligned} f = \sum_{t_p \in T_i^S} P_{I,\theta_m}(S_{t_p}) P(R = r_{t_p}^I | S_{t_p}, O = o_{t_p}^I) \\ + \sum_{t_q \in T_i^O} P_{I,\theta_m}(O_{t_q}) P(R = r_{t_q}^I | S = s_{t_q}^I, O_{t_q}) \\ = \sum_{t_p \in T_i^S} P_{I,\theta_m}(E_i) P(R = r_{t_p}^I | E_i, O = o_{t_p}^I) \\ + \sum_{t_q \in T_i^O} P_{I,\theta_m}(E_i) P(R = r_{t_q}^I | S = s_{t_q}^I, E_i) \end{aligned} \quad (22)$$

Finally we can simplify as

$$f(E_i) = P_{I,\theta_m}(E_i) \left(\sum_{t_p \in T_i^S} P(R = r_{t_p}^I | E_i, O = o_{t_p}^I) \right. \\ \left. + \sum_{t_q \in T_i^O} P(R = r_{t_q}^I | S = s_{t_q}^I, E_i) \right) \quad (23)$$

We include a pseudo-code for the constrained optimization in Algorithm 1.

Algorithm 1 Constrained Optimization For Conflict Resolution

Require: Inferred scene graph \mathcal{G}_I^{Inf} from within triplet inference with potential conflicts, maximum iteration N

```

 $\mathcal{G}_I^0 \leftarrow \mathcal{G}_I^{Inf}$ 
 $n \leftarrow 1$ 
while  $n < N$  do
  for each  $E_i \in \mathcal{G}_I^{n-1}$  do ▷ update each object value with constraints
    find triplets where  $E_i$  acts as subject and object by Eqn. 19
    modify uncertain evidences of connected triplets except  $E_i$  by Eqn. 21
    infer  $E_i^*$  by Eqn. 9
  end for
  for each  $R_j \in \mathcal{G}_I^{n-1}$  do ▷ update each relationship with updated object values
    infer  $R_j^*$  by Eqn. 10
  end for
  Construct new scene graph  $\mathcal{G}_I^n = \{\mathcal{E}^*, \mathcal{R}^*\}$ 
  if  $\mathcal{G}_I^n == \mathcal{G}_I^{n-1}$  then
    return  $\mathcal{G}_I^n$ 
  else
     $\mathcal{G}_I^{n-1} = \mathcal{G}_I^n$ 
     $n = n + 1$ 
  end if
end while

```

C Pseudo-code for sample augmentation

We include a pseudo-code for sample augmentation in Algorithm (2). The concatenation of triplet entities are done by simply adding the class labels by a ‘space’ to make it a valid sentence which can be fed into a sentence-embedding model to generate embeddings.

Algorithm 2 Sample augmentation using embedding similarity

Require: Training scene graphs \mathcal{G}^T , sentence embedding model $f(T)$ for triplet T , distance measure $\phi(f(T_a), f(T_b))$, augmentation parameter ϵ , top- N_e object entities \mathcal{N}_e , top- N_r relationships \mathcal{N}_r .

```

for each  $\mathcal{G}_i \in \mathcal{G}^T$  do
  for each  $R_j(S_j, O_j) \in \mathcal{G}_i$  do
    if  $S_j \in \mathcal{N}_e$  and  $O_j \in \mathcal{N}_e$  then
      if  $R_j \in \mathcal{N}_r$  then
         $N^a(S_j, R_j, O_j) \leftarrow N^a(S_j, R_j, O_j) + 1$ 
      else if  $R_j \notin \mathcal{N}_r$  then
         $T_i \leftarrow concat(S_j, R_j, O_j)$ 
         $dist_{min} \leftarrow \min_{T \leftarrow concat(S_j, R, O_j) \forall R \in \mathcal{N}_r} \phi(T, T_i)$ 
         $T_{min} \leftarrow \arg \min_{T \leftarrow concat(S_j, R, O_j) \forall R \in \mathcal{N}_r} \phi(T, T_i)$ 
        if  $dist_{min} < \epsilon$  then
           $S_j, R_{min}, O_j \leftarrow T_{min}$ 
           $N^a(S_j, R_{min}, O_j) \leftarrow N^a(S_j, R_{min}, O_j) + 1$ 
        end if
      end if
    end if
  end for
end for
end for
Ensure: Augmented count  $N^a(S, R, O) \forall S \in \mathcal{N}_s, \forall R \in \mathcal{N}_r, \forall O \in \mathcal{N}_o$ 

```

D Results and analysis of posterior inference with original and augmented samples

We include R@K and mR@K for all three tasks PredCls, SGCLs and SGDet for Visual Genome and GQA in Table 7. Baseline SGG models are implemented by the codebase of [26], [3], and [14]. mR@K improves in all baseline models and R@K decreases in MOTIF, VCTree, BGNN, and DLFE for VG and in all baseline models for GQA. We

also include the full comparison with the other de-biasing techniques in Table 8. We achieve better performance in all settings except in SGDet by [3].

DS	Method	Recall and Mean Recall @ K					
		PredCls		SGCls		SGDet	
		R@20/50/100	mR@20/50/100	R@ 20/50/100	mR@20/50/100	R@20/50/100	mR@20/50/100
VG	IMP [◊] [32]	54.9/ 61.6/ 63.6	9.2/ 11.5/ 12.4	32.9/ 36.1/ 37.1	4.9/ 5.7/ 6.0	21.0/ 28.0/ 31.3	3.3/ 4.9/ 5.8
	Inf-IMP (org)	55.2/ 62.5/ 64.8	15.4/ 20.5/ 22.7	33.7/ 37.3/ 38.5	7.3/ 9.32/ 10.2	20.6/ 27.3/ 30.6	4.8/ 7.6/ 9.2
	Inf-IMP (aug)	53.2/ 59.9/ 62.0	18.6/ 25.1/ 28.3	32.6/ 36.0/ 37.1	9.7/ 12.6/ 14.1	20.1/ 26.5/ 29.5	5.3/ 8.6/ 10.7
	MOTIF [◊] [42]	48.9/ 59.6/ 64.0	8.4/ 12.9/ 15.5	31.2/ 36.5/ 38.5	5.5/ 7.7/ 8.8	20.7/ 26.9/ 30.5	3.9/ 5.6/ 6.7
	Inf-MOTIF (org)	46.4/ 56.4/ 60.4	13.0/ 20.1/ 24.4	29.9/ 34.8/ 36.7	8.5/ 11.9/ 13.9	19.7/ 25.6/ 29.1	5.8/ 8.1/ 10.0
	Inf-MOTIF (aug)	42.5/ 51.5/ 55.1	15.7/ 24.7/ 30.7	27.7/ 32.2/ 33.8	10.2/ 14.5/ 17.4	18.6/ 24.0/ 27.1	6.6/ 9.4/ 11.7
	VCTree [◊] [27]	59.1/ 65.5/ 67.2	12.0/ 15.4/ 16.6	40.4/ 44.2/ 45.1	7.4/ 9.2/ 9.8	24.0/ 30.0/ 32.6	4.7/ 6.2/ 7.0
	Inf-VCTree (org)	56.6/ 62.5/ 64.1	17.7/ 22.7/ 24.8	39.3/ 42.9/ 43.8	10.7/ 13.5/ 14.6	23.4/ 29.1/ 31.6	6.3/ 8.4/ 9.5
	Inf-VCTree (aug)	54.0/ 59.5/ 61.0	21.1/ 28.1/ 30.7	37.4/ 40.7/ 41.6	13.6/ 17.3/ 19.4	22.3/ 27.7/ 30.1	7.6/ 10.4/ 11.9
GQA	Unb-MOTIF [◊] [26]	33.4/ 45.9/ 51.2	17.9/ 24.8/ 28.7	20.5/ 26.3/ 28.8	9.8/ 13.2/ 15.1	11.8/ 16.3/ 19.5	6.4/ 8.7/ 10.5
	Inf-Unb-MOTIF (org)	34.2/ 47.2/ 52.8	18.0/ 25.6/ 30.4	21.1/ 27.4/ 30.2	10.0/ 13.9/ 16.3	12.1/ 17.0/ 20.7	6.5/ 9.1/ 11.1
	Inf-Unb-MOTIF (aug)	31.5/ 42.4/ 46.8	19.2/ 28.6/ 35.7	19.0/ 24.1/ 26.3	10.7/ 15.9/ 18.9	10.9/ 15.1/ 18.0	6.6/ 9.6/ 11.9
	DLFE-MOTIF ^{lozenge} [3]	45.7/ 51.6/ 53.3	22.0/ 26.9/ 28.8	25.4/ 28.8/ 29.7	12.8/ 15.6/ 16.4	18.2/ 24.2/ 28.0	8.0/ 10.6/ 12.6
	Inf-DLFE-MOTIF (org)	49.4/ 55.7/ 57.5	25.4/ 31.4/ 33.9	27.8/ 31.2/ 32.2	14.3/ 17.5/ 18.4	20.1/ 26.5/ 30.3	9.6/ 12.7/ 14.9
	Inf-DLFE-MOTIF (aug)	38.0/ 43.3/ 44.8	28.5/ 35.3/ 38.2	21.4/ 24.3/ 25.1	16.3/ 19.7/ 20.7	15.5/ 20.6/ 23.8	10.6/ 14.1/ 16.8
	BGNN [◊] [14]	50.4/ 58.2/ 60.4	24.9/ 29.5/ 31.8	-/-/-	-/-/-	23.1/ 30.3/ 35.0	7.4/ 10.4/ 12.3
	Inf-BGNN (org)	50.2/ 57.6/ 59.8	25.4/ 30.3/ 33.1	-/-/-	-/-/-	22.1/ 28.9/ 33.4	8.5/ 12.0/ 14.5
	Inf-BGNN (aug)	48.2/ 55.4/ 57.5	26.2/ 32.2/ 34.3	-/-/-	-/-/-	20.0/ 26.2/ 30.1	9.4/ 13.2/ 16.1
GQA	IMP [◊] [32]	57.0/ 61.9/ 63.7	11.2/ 13.0/ 13.7	32.3/ 34.3/ 34.8	6.6/ 7.5/ 7.80	20.8/ 25.4/ 27.4	4.2/ 5.8/ 6.6
	Inf-IMP (org)	56.2/ 62.0/ 64.2	29.1/ 35.9/ 38.3	31.1/ 33.3/ 34.1	16.3/ 19.1/ 20.3	19.2/ 23.5/ 25.6	8.6/ 12.3/ 14.4
	Inf-IMP (aug)	56.0/ 61.9/ 64.0	28.5/ 35.1/ 37.5	31.0/ 33.2/ 34.0	16.2/ 19.1/ 20.3	19.2/ 23.5/ 25.6	8.5/ 12.2/ 14.1
	MOTIF [◊] [42]	64.0/ 68.3/ 69.7	17.5/ 20.7/ 21.6	33.2/ 34.9/ 35.4	9.8/ 10.9/ 11.3	23.9/ 27.8/ 29.4	5.8/ 7.4/ 8.3
	Inf-MOTIF (org)	59.0/ 62.9/ 64.1	31.9/ 37.8/ 39.8	30.3/ 31.9/ 32.4	16.8/ 19.0/ 19.9	21.9/ 25.5/ 26.9	11.6/ 14.4/ 15.9
	Inf-MOTIF (aug)	59.0/ 63.0/ 64.2	32.0/ 37.9/ 40.1	30.2/ 31.8/ 32.3	16.8/ 19.1/ 20.0	21.9/ 25.5/ 26.9	11.7/ 14.3/ 15.8
	VCTree [◊] [27]	64.4/ 68.8/ 70.1	18.8/ 22.1/ 23.0	33.2/ 35.0/ 35.6	9.2/ 10.6/ 11.0	23.2/ 27.2/ 28.8	5.5/ 7.0/ 7.8
	Inf-VCTree (org)	59.0/ 62.8/ 64.1	33.7/ 39.1/ 41.3	30.5/ 32.3/ 32.9	16.6/ 19.1/ 19.9	21.3/ 25.1/ 26.5	11.0/ 13.6/ 15.1
	Inf-VCTree (aug)	59.0/ 62.8/ 64.1	34.1/ 39.4/ 41.6	30.5/ 32.2/ 32.8	16.6/ 19.2/ 20.0	21.3/ 25.0/ 26.4	11.0/ 13.6/ 15.1
GQA	Unb-MOTIF [◊] [26]	43.2/ 51.9/ 55.9	19.4/ 27.8/ 32.3	21.6/ 26.1/ 28.1	10.4/ 14.1/ 16.3	13.5/ 18.2/ 21.6	7.7/ 10.8/ 12.9
	Inf-Unb-MOTIF (org)	41.4/ 50.1/ 53.9	23.1/ 34.9/ 41.3	20.6/ 24.9/ 26.9	11.9/ 17.3/ 20.7	12.5/ 16.8/ 19.9	8.7/ 12.4/ 14.8
	Inf-Unb-MOTIF (aug)	41.4/ 49.9/ 53.6	22.9/ 34.5/ 40.8	20.5/ 24.8/ 26.7	11.9/ 17.2/ 20.6	12.5/ 16.8/ 19.9	8.7/ 12.4/ 14.8

Table 7: Recall@K and Mean Recall@K results of inference with prefix ‘Inf-’. Here, (org) denotes that BN is learnt using original training samples and (aug) denotes that BN is learnt using augmented samples. \diamond – released by [26], \lozenge – released by respective authors.

D.1 Visualization of mean recall improvement

D.1.1 Quantitative

In this section, we visualize improvement of mean recall in PredCls task with measurement probabilities from VCTree [27]. In Figure 6a, we see the improvement of recalls at the tail relationships between baseline model VCTree [27] and the posterior inference with BN learnt from original data for VG dataset. In Figure 6b, we see the improvement with BN learnt from augmented samples. It is evident that augmentation helps retrieving more information from the tail relationships.

D.1.2 Qualitative

In Figure 7, a qualitative representation is shown where we see the tail relationships are improved with BN inference for different baseline models.

D.2 Ablation study on constraint satisfaction

As we discussed in Section 4.4, the conflicts of object entities after within-triplet inference of each triplets can be resolved either by simple mode selection scheme or by a constrained optimization procedure we have proposed in Section B of Appendix. The improvement with constrained optimization over mode selection is shown in Table 4.

D.3 Statistical significance test

We partition the full testing dataset into 264 folds with each fold having 100 images. For each fold, we compute the mean recall@100 in PredCls setting for baseline model [27] and for our proposed model. We perform one-sided Wilcoxon rank sum test between these two groups of performance measures and obtain $p < 0.05$ which denotes that performance increase in mean recall of our proposed method is statistically significant.

Method	Recall and Mean Recall @ K					
	PredCls		SGCls		SGDet	
	R@50/100	mR@50/100	R@50/100	mR@50/100	R@50/100	mR@50/100
VCTree[27]	65.5/ 67.2	15.4/ 16.6	44.2/ 45.1	9.2/ 9.8	29.9/ 32.6	6.2/ 7.0
Unb-VCTree [26]	47.2/ 51.6	25.4/ 28.7	25.4/ 27.9	12.2/ 14.0	19.4/ 23.2	9.3/ 11.1
DLFE-VCTree [3]	51.8/ 53.5	25.3/ 27.1	28.0/ 28.9	18.2/ 19.0	22.6/ 26.2	11.7/ 13.6
Inf-VCTree (Ours)	59.5/ 61.0	28.1/ 30.7	40.7/ 41.6	17.3/ 19.4	27.7/ 30.1	10.4/ 11.9

Table 8: Comparison with other de-biasing methods in all settings

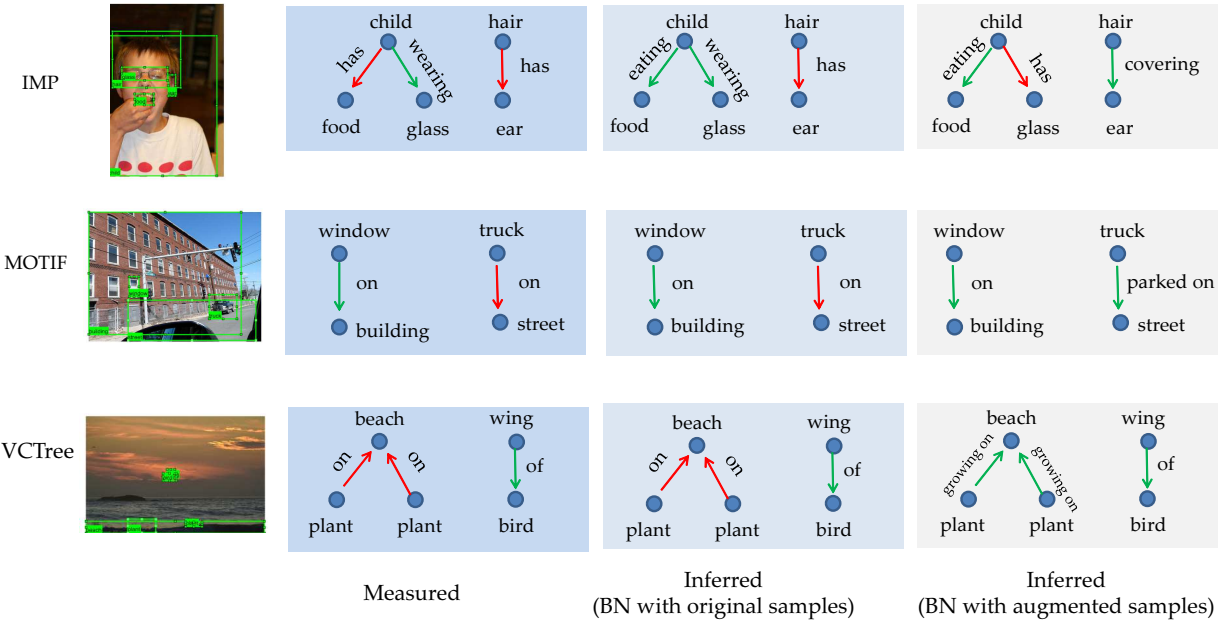


Figure 7: Improvement of tail relationships for IMP [32], MOTIF [42], and VCTree [27]. We visualize the improvement of inference with BN learnt from both original and augmented samples. This is a PredCls setting where we know the object locations and classes. The red arrow indicates incorrect relationship, and green arrow indicates correct relationships